ELSEVIER

Biochimica et Biophysica Acta 1567 (2002) 143–149

BIOCHIMICA ET BIOPHYSICA ACTA
BBA

www.bba-direct.com

Syringotoxin pore formation and inactivation in human red blood cell and model bilayer lipid membranes

Zsófia Szabó[a], Pál Gróf[a], Ludmila V. Schagina[b], Philip A. Gurnev[b], Jon Y. Takemoto[c], Edit Mátyus[a], Katalin Blaskó[a,*]

[a] *Institute of Biophysics and Radiation Biology, Semmelweis University Budapest, Bupapest VIII, Puskin u. POB 263, H-1444 Budapest, Hungary*
[b] *Institute of Cytology, Russian Academy of Sciences, St. Petersburg, Russia*
[c] *Department of Biology, Utah State University, Logan, UT, USA*

Received 8 January 2002; received in revised form 16 July 2002; accepted 24 September 2002

Abstract

The effect of syringotoxin (ST), a member of the cyclic lipodepsipeptides family (CLPs) produced by *Pseudomonas syringae* pv. *syringae* on the membrane permeability of human red blood cells (RBCs) and model bilayer lipid membranes (BLMs) was studied and compared to that of two recently investigated CLPs, syringomycin E (SRE) and syringopeptin 22A (SP22A) [Biochim. Biophys. Acta 1466 (2000) 79 and Bioelectrochemistry 52 (2000) 161]. The permeability-increasing effect of ST on RBCs was the least among the three CLPs. A time-dependent ST pore inactivation was observed on RBCs at 20 and 37 °C but not at 8 °C. From the kinetic model worked out parameters as permeability coefficient of RBC membrane for $^{86}Rb^{+}$ and pores mean lifetime were calculated. A shorter pores mean lifetime was calculated at 37 °C then at 20 °C, which gave us an explanation for the unusual slower rate of tracer efflux measured at 37 °C then that at 20 °C. The results obtained on BLM showed that the pore inactivation was due to a decrease in the number of pores but not to a change of their dwell time or conductance.

Keywords: Syringotoxin; Pore formation; Pore inactivation; Transport model; Red blood cell; Model bilayer lipid membrane

1. Introduction

The widespread phytopathogen *Pseudomonas syringae* pv. *syringae* produces toxic cyclic lipodepsipeptides (CLPs). There are two groups of CLPs, the first group includes the nonapeptides: syringomycins (SRs) [1–3], syringotoxin (ST) [4], syringostatins [1] and pseudomycins [5], while the second includes the larger syringopeptins (SPs) [6]. The CLPs have a charged cyclic peptide head and a hydrophobic 3-hydroxy-fatty acid tail of variable length. The most studied CLP, nonapeptide syringomycin E (SRE) also possesses a peptide lactone ring, with three positive and one negative charges and 3-hydroxy-dodecanoic acid hydrocarbon tail. The syringopeptins contain a peptide moiety composed of 22 (SP22A, SP22B) or 25 (SP25A, SP25B) amino acid residues from which the last eight ones form a lactone ring, with two positive charges. The fatty acid moiety is either 3-hydroxydecanoic (SP22A, SP25A) or 3-hydroxydodecanoic acid (SP22B, SP25B).

CLPs have both phytotoxic [7,8] and antimicrobial effects [9]. However, the syringopeptins have stronger phytotoxic activities than the nonapeptides [9,10]. All CLP derivatives inhibit the growth of fungi, although different fungal species display different degrees of sensitivity [9,11]. The antifungal activities are affected by membrane composition, especially sphingolipids and sterols [12–15]. Lipid involvement in CLP action was also shown with bilayer lipid membranes (BLM) and human red blood cells (RBC) [16,17]. Several Gram-negative bacteria were unaffected by CLPs, while Gram-positive bacteria were found to have variable sensitivities to the CLPs [9].

CLPs induce lysis of RBCs and tobacco protoplasts presumably due to the colloid osmotic shock provoked by the ion flux through pores [18]. Hutchison et al. [19] found that SRs and SPs have equivalent activities on tobacco protoplasts while Lavermicocca et al. [9] reported that SPs

* Corresponding author. Tel.: +36-1-266-6656; fax: +36-1-266-6656.
E-mail address: blasko@puskin.sote.hu (K. Blaskó).

0005-2736/02/$ - see front matter © 2002 Elsevier Science B.V. All rights reserved.
PII: S0005-2736(02)00610-7

were more active on potato tuber discs than were SRE and ST. Dalla Serra et al. [20] compared the hemolytic effect of CLPs on human and rabbit RBCs and found that the most effective was SRE, less effective was the ST and the weakest were the SPs. Hutchison et al. [19] observed that SPs were 85% as effective as SRE on horse erythrocytes. In contradiction, Lavermicocca et al. [9] reported that SPs have the highest lytic activities, SRE was less effective and the least active was ST on sheep RBCs in agreement with Sorensen et al. [11].

The primary target of the CLPs is the plasma membrane, altering several of its functions such as ion transport, K^+–H^+–ATPase activity, and membrane potential [21–23]. All these effects are suggested to be the consequence of the membrane pore-forming activities of CLPs. [19,20,24]. Pore formation in BLMs has been extensively analyzed with SRE and SP22A [25–27]. Two types of channels, large and small, were registered by single channel recording with incorporation of either SRE or SP22A into BLM [25–28]. The large channels are clusters of six small ones, and the radii of the channel aqueous pores in both small and large channels are approximately equal to 1 nm [25]. Dalla Serra et al. [20] also suggested that SRE and SP22A form oligomeric pores. SRE induced a large integral current that remained stable at 14 °C, but at 23 °C decreased over time while the single channel conductance and dwell time did not change. This indicated a temperature-dependent inactivation of SRE pores due to a decrease in the number of pores [26]. On the contrary, no pore inactivation was observed with SP22A, and a constant integral current was measured for as long as 2.5 h [27]. The channel-forming activity of SP22A was found to be about one order of magnitude higher than that of SRE [27]. A higher pore-forming activity of SP22A vs. SRE and a temperature-dependent pore inactivation with SRE, but not with SP22A were also observed in human RBCs [27].

SRE and SP22A clearly display different pore-forming properties. Although the molecular basis for these differences is not known, it is likely that they are due to differences in molecular charge or hydrophobicity or a combination of both. In the present work, studies with ST were undertaken to specifically assess the contribution of molecular charge to the CLP pore formation mechanism. ST uniquely possesses a glycine residue in place of a basic amino acid found in the other known nonapeptide CLPs. As a consequence, ST has one less positive charge than the other CLPs. The pore forming and inactivation activities of ST were studied and compared to those previously reported for SRE and SP22A.

2. Materials and methods

Human blood from healthy volunteers was stabilized with citrate buffer and stored at 4 °C, up to 3 days. Synthetic 1,2-dioleoyl-*sn*-glycero-3-phosphoserine (DOPS) and 1,2-dioleoyl-*sn*-glycero-3-phosphoethanolamine (DOPE) were purchased from Avanti Polar Lipids, Inc., Pelham, AL, USA. ST was purified to homogeneity by previously published methods [29] from cultures of *P. syringae* strain PS268 [30] obtained from D.C. Gross (Texas A&M University, College Station, TX, USA). All chemicals used were of analytical grade.

2.1. $^{86}Rb^+$ efflux from human RBCs

Blood was loaded with $^{86}Rb^+$ for 100 min at 37 °C. After centrifugation, RBCs were washed three times with buffered salt (BS) solution: (in mmol/l: 3.2 KCl, 138 NaCl, 1 $CaCl_2$, 1 $MgCl_2$, 27 glucose, buffered with 3-(N-morpholino)-propanesulfonic acid (MOPS) for pH 6.8), and then re-suspended in the BS solution to achieve a hematocrit value (H) between 0.4 and 0.5. RBC suspensions were kept either at 37 °C or chilled to temperatures 8 °C or 20 °C and kept at this temperature.

ST stock solution (1 mg/ml in 10^{-3} mol/l HCl) was diluted with 6 ml of BS solution. Diluted ST solution and RBC suspension (14 ml) was mixed with rigorous stirring. The final ST concentrations (c_{ST}) were in the range of $2 \times 10^6 - 1.3 \times 10^7$ molecules/cell (39.4–256.3 μg/ml RBCs). The RBC suspensions were incubated at a given temperature (8, 20 or 37 °C) in a shaking water bath. Samples of the suspension were taken at designated time intervals, centrifuged and the radioactivities of the supernatant aliquots were measured with a γ-scintillation counter (Gamma, Budapest, Hungary).

$^{86}Rb^+$ transport was characterized by the amount of tracer found in the supernatant fluids after a time period t and expressed as the percentage of the total activity of the suspension (N_t). Tracer efflux was plotted in a curve N_t vs. (t), as well as in a semilogarithmic representation: $-\ln(1-(N_t-N_o)/(N_\infty-N_o))$ over time, where N_o denote the percentage value of $^{86}Rb^+$ in the external medium at $t=0$ due to contamination and lysis and N_∞ is the percentage amount of $^{86}Rb^+$ in the extracellular solution at tracer equilibrium between the intra- and extracellular spaces. RBC concentration and hematocrit values were determined using an automated hematology analyzer (COBAS MICROS OT 18, Roche, France). The ST-induced hemolysis was calculated as the difference between the RBC concentrations of the untreated (A_o) and ST-treated (A) RBC suspensions and expressed as a percentage of A_o.

2.2. Hemoglobin efflux from human RBCs

The extracellular hemoglobin (Hgb) concentration was determined in cyanmethemoglobin form by measuring the optical density (OD) at $\lambda = 545$ nm with a spectrophotometer (Perkin-Elmer-Lambda 15 UV–VIS), and expressed in the percentage of the total hemoglobin content of the RBC suspension (Hgb%). Hemoglobin transport was presented in a Hgb% vs. t curve.

2.3. Measurements of single channel current and conductance on BLM

Virtually solvent-free membranes were prepared as described by Montal and Mueller [31]. Bilayer membranes were formed from an equimolar mixture of DOPS and DOPE in pentane. The BLM was bathed in 100 mmol/l NaCl, 5 mmol/l MOPS (pH 6). Two symmetrical halves of a Teflon chamber with solution volumes of 1.5 cm^3 was divided by a 10-μm-thick Teflon partition containing a round aperture of about 100 μm diameter. Squalene was used for aperture pretreatment. A pair of Ag–AgCl electrodes was used to maintain membrane potential and to detect current fluctuations. "Virtual ground" was maintained at the *trans* side of the bilayer. Positive currents are therefore those of cations flowing from *cis* to *trans*. For unmodified bilayers, a conductance value smaller than 1 pS was found which remained unchanged during several hours. ST was added to the aqueous phase at one (*cis*) side of the bilayer from stock solutions (1 mg/ml in 10^{-3} mol/l HCl). Details on membrane preparation, single channel and membrane current measurements may be found elsewhere [32].

3. Results and discussions

The lytic and the membrane permeability-increasing effects of ST applied in the concentration range of 2×10^6–13×10^6 molecules/cell were investigated at different temperatures: 8, 20 and 37 °C. At all of these concentrations and temperatures, ST caused weak lysis with less than 6% of cells undergoing lysis. On the other hand, ST increased the membrane permeability for $^{86}Rb^+$ and hemoglobin only above the concentration of 6×10^6 molecules/cells and in a concentration-dependent manner.

Fig. 1 shows typical time courses of ST-induced $^{86}Rb^+$ (Fig. 1A) and hemoglobin (Fig. 1B) effluxes measured at 20 °C at two different ST concentrations (7.2×10^6 and 1×10^7 molecules/cell). Although the $^{86}Rb^+$ and hemoglobin effluxes increased in time after addition of the toxin, the equilibrium of tracer and hemoglobin distributions between the intra- and extracellular spaces was not achieved during the time period of the experiment (150 min). The transport curves approached saturation levels well before equilibrium was achieved.

The effect of temperature on the ST-induced $^{86}Rb^+$ efflux at a ST concentration of about 1×10^7 molecules/cell is presented in Fig. 2A. The transport curves obtained at 20 and at 37 °C showed similar kinetics. The saturation level of the efflux observed at 37 °C was also far from the equilibrium tracer distribution. Similar results obtained earlier with SRE were suggested to be due to a time- and temperature-dependent pore inactivation [17,26,27]. With ST, however, a surprising observation was that $^{86}Rb^+$ efflux measured at 20 °C was more rapid than that at 37 °C, even when applied at higher concentration (1.3×10^7 molecules/cell) at 37 °C than at 20 °C (1.0×10^7 molecules/cell). A similar result was obtained with Hgb efflux (data not shown). At 8 °C, the $^{86}Rb^+$ efflux increased gradually and approached the equilibrium tracer distribution. A semilogarithmic representation of the effects at 8 °C (Fig. 2B) showed a straight line indicating first-order kinetics and a free diffusion of ions through water-filled pores without detectable pore inactivation for as long as 60 min. In contrast, no such efflux kinetics was observed at 20 and 37 °C. Thus, at room and body temperatures, it is suggested that temperature-dependent ST pore inactivation occurs. In this respect, the ST pores seem to be similar to SRE pores

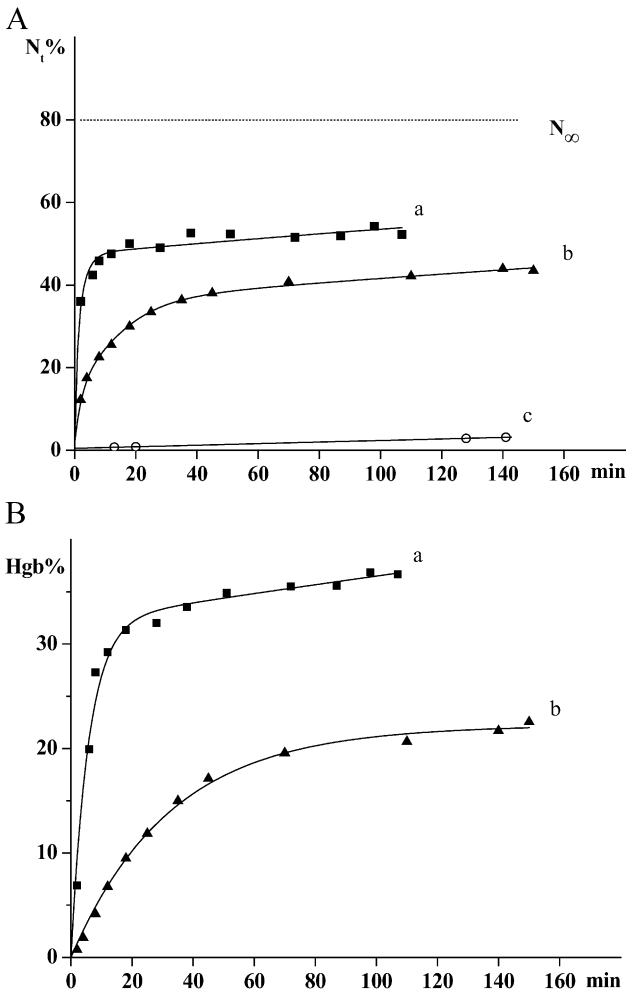

Fig. 1. (A) Time course of ST-induced $^{86}Rb^+$ efflux through RBC membrane. RBCs were suspended in BS solution (in mmol/l: 3.2 KCl, 138 NaCl, 1 $MgCl_2$, 27 glucose 5 MOPS (pH 6.8), temperature 20 °C). The ordinate gives the amount of effluxed tracer expressed as the percentage of the total activity of the RBC suspension (N_t). N_∞ is the percentage amount of $^{86}Rb^+$ in the extracellular solution at tracer equilibrium between the intra- and extracellular spaces. ST concentrations in molecules/cell (μg/ml): (a) 1×10^7 (197); (b) 7.2×10^6 (142); (c) 0, ST was added at 0 min. Solid lines are fitted curves calculated by help of the kinetic model. (B) Time course of ST-induced Hgb efflux through RBC membrane. The ordinate gives the amount of effluxed Hgb expressed in the percentage of the total Hgb content of the RBC suspension. For experimental conditions, see panel A. Solid lines are fitted curves calculated with the help of the kinetic model.

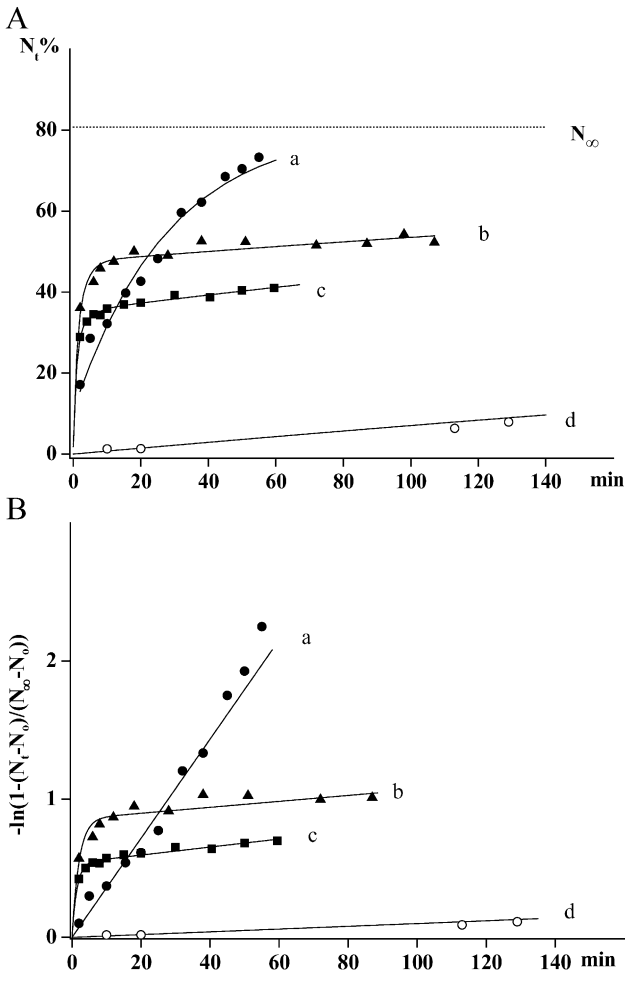

Fig. 2. (A) Temperature dependence of ST-induced $^{86}Rb^+$ efflux through RBC membrane. RBCs were suspended in BS solution (for composition, see Fig. 1). The ordinate gives the amount of effluxed tracer, expressed as the percentage of the total activity of the RBC suspension (N_t). N_∞ is the percentage amount of $^{86}Rb^+$ in the extracellular solution at tracer equilibrium between the intra- and extracellular spaces. Temperatures: (a) 8 °C; (b) 20 °C; (c) 37 °C; (d) 37 °C. ST concentrations in molecules/cell (μg/ml): (a) 1.28×10^7 (256); (b) 1×10^7 (197); (c) 1.27×10^7 (256); (d) 0. ST was added at 0 min. Solid lines are fitted curves calculated with the help of the kinetic model. (B) Semilogarithmic representation of kinetic data given in panel A. Solid lines are fitted curves calculated with the help of the kinetic model.

[26], e.g. they inactivate at body and at room temperatures but not at low temperature (6–8 °C) where the major lipids of the RBC membranes are in gel phase [17,26]. On the contrary, SP22A displays first-order kinetics of tracer and hemoglobin transport at 37 °C suggesting no pore inactivation [27].

Pore inactivation may result from a decrease in number of pores, reduction of single channel conductance, or a decrease of open state channel dwell time. To determine which of these mechanisms applies to ST pore inactivation, studies were conducted with planar lipid bilayers made with mixtures of phosphatidylserine and phosphatidylethanolamine. These phospholipids are negatively charged and neutral lipid components of the RBC membrane, respectively. Fig. 3 shows the time course of the integral conductance of the BLM in the presence of ST measured at 24 °C. The integral transmembrane conductance measured at a positive potential increased gradually after addition of ST to a maximum in 2.5 min and then began to decrease thereafter. Single channel recordings showed that conductance of single channels and their dwell time did not change over time (Fig. 4A and B). This indicates that the decrease of the macroscopic conductance is due to a marked decrease in the number of pores rather than to a reduction of a single pore conductance or dwell time. As with SRE [25,33] and SP22A [27] two types of pores (small and large ones) were registered with single channel recordings on ST-treated BLMs (Fig. 4). The ratio of conductance for ST-induced small and large channels was found to be in the range of 4–5. As with SRE or SP22A, the application of negative potential to ST-treated BLM induced closing of the channels (data are not shown). These findings suggest a similar mechanism of channel formation for ST, SRE and SP22A. The single channel conductivity, the channel gating properties, and their dependence on the salt concentration in the bathing solution, as well as on the lipid composition of the BLM were found to be very similar for the three CLPs [26,27,34]. It is reasonable to suppose that the ST pore possesses similar physical dimensions as SRE and SP22A of about 1 nm pore radius. Finally, it is likely that hemoglobin is transported through the ST pores (Fig. 1B) in monomeric form as suggested for SRE pores [17].

To understand the unusual higher transport rates of $^{86}Rb^+$ and hemoglobin measured at 20 °C than at 37 °C a kinetic model was worked out (see Appendix A). The pores mean lifetime, τ_{inact} ($\tau_{inact} = 1/k_{inact}$) calculated at 8 °C exceeded 60 min, the time course of the experiment proving the

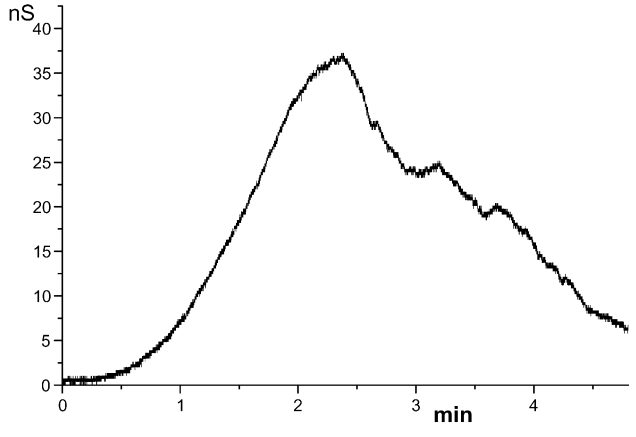

Fig. 3. Time course of the integral conductance of the bilayer doped with ST at an applied voltage of 100 mV. Membrane was formed from a lipid mixture of DOPS/DOPE (1:1, M/M). Membrane bathing solutions contained 100 mmol/l NaCl (pH 6). Temperature was 24 °C. ST was added to the bathing solution at the *cis* side only at a concentration of 20 μg/ml.

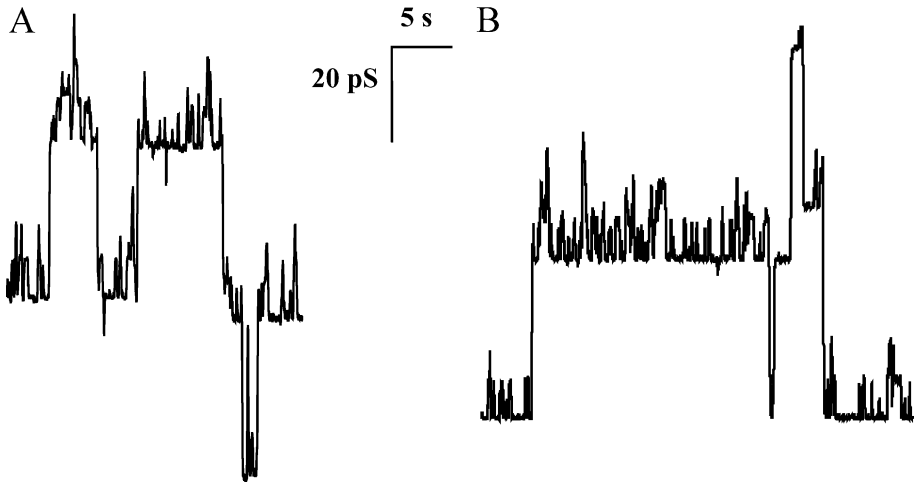

Fig. 4. Records of current fluctuations at −175 mV transmembrane potential difference in ST modified bilayers in 1.5 min (A) and 10 min (B) after ST addition. For other conditions, see Fig. 3.

absence of ST pore inactivation at this temperature (Table 1). The obtained τ_{inact} values at 37 °C were less, while at 20 °C more than 2 min. This finding explained the observed lower transport rate at 37 °C than at 20 °C already at the first measured time point of the transport. That is why the rate constant of $^{86}Rb^+$ efflux through the pores (k_p) was not possible to read directly from the transport curve. By means of the model, however, k_p was determined and permeability coefficient for $^{86}Rb^+$ (p_p) was calculated [27] (Table 1). Correlation between the logarithm of p_p and ST concentration was used to attempt the determination of the number of monomers involved in a single pore which is given by the slope of the curve in such a representation [35,36]. ST pores were found to be oligomers of 2–6 (4.2 ± 1.8) monomers.

An interesting feature of the temperature dependence of p_p values is that in the temperature range of 8–20 °C, a Q_{10} value >10 is obtained as compared to Q_{10} = 1.2–1.3 for free diffusion of $^{86}Rb^+$ through water-filled pores [37]. The high Q_{10} value may be a result of increasing numbers of ST pores in the membranes with increasing temperature, suggesting temperature-dependent pore forming activity of ST.

Table 1
Kinetic parameters of the ST-induced $^{86}Rb^+$ transport calculated by the model

T (°C)	c_{ST} (molecule/cell)	τ_{inact} (min)	p_p (cm/s)
8	5.80e+06	297	3.17e−10
	6.50e+06	268	2.84e−09
	8.80e+06	79.5	8.73e−09
	1.00e+07	∞	1.51e−09
	1.28e+07	∞	2.22e−08
20	6.91e+06	4.1	3.77e−08
	7.16e+06	10.4	3.08e−08
	8.73e+06	2.3	1.99e−07
	9.98e+06	2.0	2.17e−07
37	5.77e+06	1.7	8.52e−08
	9.06e+06	1.7	1.64e−07
	9.37e+06	1.9	1.28e−07
	1.19e+07	1.1	3.30e−07
	1.27e+07	1.4	2.45e−07

τ_{inact} is the pores mean lifetime; p_p is the permeability coefficient for $^{86}Rb^+$.

The faster inactivation of ST pores than SRE pores and the lack of it in case of SP22A may be considered in light of their structural differences. SP22A is about twice the size of ST and SRE and its hydrophobic character is the strongest of the three. SRE and ST possess less and nearly equal hydrophobicity. SP22A and SRE have two net positive charges, and ST has one. One may speculate that pore inactivation is an irreversible structural transformation in a structure which does not provide a pathway for ions. One such structure could be something like an inverted micelle in which the CLP acyl chains interact with the apolar tails of phospholipid molecules, and the polar CLP head groups interact with one another so that the charges of the molecules will affect the formation of this structure. The stronger repulsive positive charges of SRE vs. ST may counteract formation of this structure, and as a result, ST pore inactivation would be a faster process than SRE pore inactivation. With SP22A, however, no observable pore inactivation was obtained even at body temperature [27]. SP22A would invoke a stronger hydrophobic effect with the hydrocarbon chains of the lipid molecules in addition to strong head group charge repulsions so that altogether the probability of SP22A pore inactivation would be decreased.

Acknowledgements

The authors gratefully thank to Dr. K. Módos for the fruitful discussion on the kinetic model and to Ms. Á. Iszlai and Mrs. A. Wolf for the skilled technical assistance. This research was supported by grants from the Hungarian

Ministry of Health (ETT: 486/96; ETT: 229/2000), the Russian Fund for Basic Research (No. 00-04-49386 and No.01-04-06290, and funds from the Utah Agricultural Experiment Station (project UTA 607).

Appendix A

Here we formulate a kinetic model for the ST-induced transport of the $^{86}Rb^{+}$ ions from the RBCs and demonstrate that this model can be generalized to describe similar transport processes.

A.1. Kinetic model of ST-induced ion transport

We assume that two paths realize the transport of the $^{86}Rb^{+}$ ions through the membrane: (1) the non-modified portion of membrane and (2) ST pores. Both of them can be described by first-order kinetics. For the non-modified portion of membrane, this assumption is obviously true, hence the transport is a passive process directed by only the chemical potential gradient between the two sides of the membrane. On the other hand, the result of interaction of ST with the RBC membrane is the pore formation, which gives a pathway for passive ion diffusion. Since there is no other biochemical reaction involved in the interaction, which may influence the ion transport process through the ST-treated RBC membrane, the efflux through the pores can also be described by a first-order kinetics. We can conclude from the above consideration that the total efflux through the membrane can be described by a first-order competitive kinetics, characterized by the rate constants k_{nm} and k_p. The first rate constant describes the transport through the non-modified portion of membrane and the second one would account for the transport through the pores. In agreement with the experimental observations that the pore formation had been completed before the first measured efflux data, we suppose an infinitely fast pore formation, so no time-dependent pore formation is taken into account.

The time course of the ion transport (Fig. 1A) suggests a time-dependent decrease of the pores' contribution to the overall efflux due to the pore inactivation. We suppose a first-order kinetics for the inactivation of the pores, which can be characterized by the rate constant, k_{inact}, or by the pores mean lifetime, $\tau_{inact} = 1/k_{inact}$. Further, we suppose that when pores inactivate, the re-created poreless membrane contributes to the overall transport with the same characteristics as the non-modified membrane. This latter supposal corresponds to the experimental observation, that at longer time, $t \gg \tau_{inact}$, the measured $^{86}Rb^{+}$ transport decreases to the order of magnitude of the non-modified membrane. To characterize the contributions of the pores and non-modified membrane to the total efflux, the two membrane portions as effective cross-sections, x_p and x_{nm} are defined. According to the above, the sum of x_p and x_{nm} is equal to one at each time point. Let us suppose that pores, which are formed at, time $t=0$ in a portion of x_{po} decreases to a value of $x_{p\infty}$ at $t \to \infty$ due to inactivation. Thus, the time dependence of the effective cross-sections, x_p and x_{nm}, can be described as:

$$x_p = x_{p\infty} + (x_{po} - x_{p\infty})\exp(-k_{inact}t) \quad (1)$$

and accordingly:

$$x_{nm} = 1 - x_p.$$

Let us denote the amount of tracer in the intracellular space at a given time t by $N(t)$. The efflux rate of the tracer ($dN(t)/dt$) from the cells can be written as:

$$\frac{dN(t)}{dt} \propto -x_p k_p N(t) - x_{nm} k_{nm} N(t), \quad (2)$$

where the first term describes the efflux of the tracer from the cells through the pores, and the second term is the efflux through the non-modified portion of membrane. Thus, the rate of tracer flux towards the extracellular space of RBCs is: $dN_t/dt = -dN(t)/dt$, where N_t is the amount of tracer in the extracellular space.

Using Eqs. (1) and (2), N_t can be expressed as:

$$N_t = N_o + (N_\infty - N_o)\left\{1 - \exp(-(k_{nm} + (k_p - k_{nm})x_{p\infty})t) \times \exp\left[-(k_p - k_{nm})(x_{po} - x_{p\infty})\frac{[1 - \exp(-k_{inact}t)]}{k_{inact}}\right]\right\} \quad (3)$$

As a consequence of the time-dependent inactivation and the coupling between x_{nm} and x_p, one cannot divide the complete solution of Eq. (3) into two separate solutions: one for the non-modified portion of membrane and other for the ST-pores.

In order to find the solution for Eq. (3), a non-linear least square fitting was applied. For x_p and x_{nm}, negative or greater than 1 values were not allowed. For the fitting procedure ensuring the highest possible range for x_p, and k_{nm} values, similar to those obtained from experimental data, the following seed values were chosen: $x_{po} = 0.99$; $x_{p\infty} = 0.1$; $k_p = 0.1\ min^{-1}$; $k_{nm} = 0.0005\ min^{-1}$; $\tau_{inact} = 10$ min and $N_o = 0.01$.

Using the above model, we calculated the fitted curves to each of the experiments, and determined the appropriate rate constants, k_{nm} and k_p, and the pore mean lifetimes, τ_{inact}. Then the permeability coefficient, p_p, for $^{86}Rb^{+}$ was calculated [27] from the k_p; p_p characterizes the permeability of RBC membranes due to pores.

A.2. Generalization of the model

The model worked out can be used to describe the ion transport induced by any other pore-forming compounds when the criteria of this model are met. These are:

(a) transport of the chosen molecule through both the non-modified membrane and the pores can be characterized by first-order kinetics;
(b) pore formation is infinitely fast, so that its time dependence should not to be taken into account;
(c) pores inactivate according to a first-order kinetics;
(d) inactivation of the pores leads to a membrane with identical characteristics as the non-modified one.

List of symbols

$N(t)$	the amount of $^{86}Rb^+$ in the internal space of RBCs at time t expressed as the percentage of the total activity of the RBC suspension
N_t	the amount of $^{86}Rb^+$ in the external medium after time period t expressed as the percentage of the total activity of the RBC suspension
N_o	the amount of $^{86}Rb^+$ in the external medium due to contamination and lysis expressed as the percentage of the total activity of the RBC suspension
N_∞	the percentage amount of $^{86}Rb^+$ in the extracellular solution at tracer equilibrium between the intra- and extracellular spaces
Hgb%	the amount of hemoglobin in the external medium expressed as the percentage of the total hemoglobin content of the RBC suspension
x_p	effective cross-section for the transport through the pores
x_{nm}	effective cross-section for the transport through non-modified portion of membrane
k_{nm}	rate constant of $^{86}Rb^+$ efflux through non-modified membrane
k_p	rate constant of $^{86}Rb^+$ efflux through the pores
k_{inact}	rate constant of pore inactivation in RBC membrane
t	running time
τ_{inact}	pores mean lifetime
p_p	permeability coefficient for $^{86}Rb^+$

References

[1] N. Fukuchi, A. Isogai, J. Nakayama, S. Takayama, S. Yamashita, K. Suyama, J.Y. Takemoto, A. Suzuki, J. Chem. Soc., Perkin Trans. 1 (1992) 1149–1157.
[2] E. Vaillo, A. Ballio, P.-L. Luisi, R.M. Thomas, Biopolymers 32 (1992) 1317–1326.
[3] A. Segre, R.C. Bachmann, A. Ballio, F. Bossa, I. Grgurina, N.S. Iacobellis, G. Marino, P. Pucci, M. Simmaco, J.Y. Takemoto, FEBS Lett. 255 (1989) 27–31.
[4] A. Ballio, F. Bossa, A. Collina, M. Gallo, N.S. Iacobellis, M. Paci, P. Pucci, A. Scaloni, A. Segre, M. Simacco, FEBS Lett. 269 (2) (1990) 377–380.
[5] A. Ballio, F. Bossa, D. Di Giorgio, P. Ferranti, M. Paci, P. Pucci, A. Scaloni, A. Segre, G.A. Strobel, FEBS Lett. 355 (1) (1994) 96–100.
[6] A. Ballio, D. Barra, F. Bossa, A. Collina, I. Grgurina, G. Marino, G. Moneti, M. Paci, P. Pucci, A. Segre, M. Simmaco, FEBS Lett. 291 (1991) 109–112.
[7] N.S. Iacobellis, P. Lavermicocca, I. Grgurina, M. Simmaco, A. Ballio, Physiol. Mol. Plant Pathol. 40 (1992) 107–116.
[8] D.C. Gross, J.E. DeVay, Physiol. Plant Pathol. 11 (1977) 1–11.
[9] P. Lavermicocca, N. Sante Iacobellis, M. Simmaco, A. Graniti, Physiol. Mol. Plant Pathol. 50 (1997) 129–140.
[10] D. Di Giorgio, L. Camoni, K.A. Mott, J.Y. Takemoto, A. Ballio, Plant Pathol. 45 (1996) 564–571.
[11] K.N. Sorensen, K.H. Kim, J.Y. Takemoto, Antimicrob. Agents Chemother. 40 (1996) 2710–2713.
[12] R. Wangspa, J.Y. Takemoto, FEMS Microbiol. Lett. 167 (1998) 215–220.
[13] C. Julmanop, Y. Takano, J.Y. Takemoto, T. Miyakawa, J. Gen. Microbiol. 139 (1993) 2323–2327.
[14] H. Hama, D.A. Young, J.A. Radding, D. Ma, J. Tang, S.D. Stock, J.Y. Takemoto, FEBS Lett. 478 (1–2) (2000) 26–28.
[15] S.D. Stock, H. Hama, J.A. Radding, D.A. Young, J.Y. Takemoto, Antimicrob. Agents Chemother. 44 (5) (2000) 1174–1180.
[16] A.M. Feigin, L.V. Schagina, J.Y. Takemoto, J.H. Teeter, J.G. Brand, Biochim. Biophys. Acta 1324 (1997) 102–110.
[17] K. Blasko, L.V. Schagina, G. Agner, Yu.A. Kaulin, J.Y. Takemoto, Biochim. Biophys. Acta 1373 (1998) 163–169.
[18] G. Menestrina, G. Schiavo, C. Montecucco, Mol. Aspects Med. 15 (1994) 179–193.
[19] M.L. Hutchison, D.C. Gross, Mol. Plant-Microb. Interact. 10 (1997) 347–354.
[20] M. Dalla Serra, G. Fagiuoli, P. Nordera, I. Bernhart, C. Della Volpe, D. Di Giorgio, A. Ballio, G. Menestrina, Mol. Plant-Microb. Interact. 12 (5) (1999) 391–400.
[21] H.H. Reidl, J.Y. Takemoto, Biochim. Biophys. Acta 898 (1987) 59–69.
[22] H. Batoko, A. de Kerchove-d'Exaerde, J.M. Kinet, J. Bouharmont, R.A. Gage, H. Maraite, M. Boutry, Biochim. Biophys. Acta 1372 (2) (1998) 216–226.
[23] F.S. Che, K. Kasamo, N. Fukuchi, A. Isogai, A. Suzuki, Physiol. Plant 86 (1992) 518–524.
[24] M.L. Hutchison, M.A. Tester, D.C. Gross, Mol. Plant-Microb. Interact. 8 (1995) 610–620.
[25] Yu.A. Kaulin, L.V. Schagina, S.M. Bezrukov, V.V. Malev, A.M. Feigin, J.Y. Takemoto, J.H. Teeter, J.G. Brand, Biophys. J. 74 (1998) 2918–2925.
[26] G. Agner, Yu.A. Kaulin, L.V. Schagina, J.Y. Takemoto, K. Blasko, Biochim. Biophys. Acta 1466 (2000) 79–86.
[27] G. Agner, Yu.A. Kaulin, P.A. Gurnev, Zs. Szabo, L.V. Schagina, J.Y. Takemoto, K. Blasko, Bioelectrochemistry 52 (2000) 161–167.
[28] A.M. Feigin, J.Y. Takemoto, R. Wangspa, J.H. Teeter, J.G. Brand, J. Membr. Biol. 149 (1996) 41–47.
[29] P. Bidwai, L. Zhang, R.C. Bachmann, J.Y. Takemoto, Plant Physiol. 83 (1987) 39–43.
[30] D.C. Gross, J.E. De Vay, F.H. Stadtman, J. Appl. Bacteriol. 43 (1977) 453–463.
[31] M. Montall, P. Mueller, Proc. Natl. Acad. Sci. U. S. A. 69 (1972) 3561–3566.
[32] S.M. Bezrukov, I. Vodyanoy, Biophys. J. 64 (1993) 16–25.
[33] L.V. Schagina, Yu.A. Kaulin, A.M. Feigin, J.Y. Takemoto, J.G. Brand, V.V. Malev, Membr. Cell Biol. 12 (4) (1998) 537–555.
[34] Ph.A. Gurnev, Yu.A. Kaulin, R. Wangspa, J.Y. Takemoto, V.V. Malev, L.V. Schagina, Cytologia 44 (3) (2002) 296–304 (in Russian).
[35] A. Finkelstein, R. Holz, in: G. Eisenman (Ed.), Membranes, Dekker, New York, 1973, pp. 377–408, r. 2.
[36] R. Latorre, O. Alvares, Physiol. Rev. 61 (1981) 77–150.
[37] B. Hille, Ionic Channels of Excitable Membranes, Sinauer Associates, Sunderland, MA, 1984, p. 426.